*Transactions of the Materials Research Society of Japan* 25 [3] 845-847 (2000)

# Nano-scale patterning of GaAs using local probe oxidation technique

Yoshimasa Iuchi, Mitsuo Kawabe, and Yoshitaka Okada
Institute of Applied Physics, University of Tsukuba, 1-1-1 Tennodai, Tsukuba 305-8573, Japan
Fax: +81-298-53-5205, E-mail: okada@bk.tsukuba.ac.jp

Some basic properties of GaAs oxides generated by using the local probe nano-oxidation process have been investigated. A scanning microprobe X-ray photoelectron spectroscopy (XPS) analysis has revealed that the main constituents of the GaAs anodic oxide were $Ga_2O_3$ and $As_2O_3$. The electrical characterization has shown that the electron transport across a GaAs oxide nano-dot of a given thickness, from a doped $n^+$-Si tip into the $n^+$-GaAs(100) substrate, over a range of applied bias, can be fitted by the Fowler-Nordheim tunneling mechanism.
Keywords: scanning probe microscope, atomic force microscope, tip-induced oxidation, anodic oxide, GaAs

## 1. INTRODUCTION

The scanning probe microscopes (SPMs) have been used to produce the structural, chemical and electronic modifications to the substrate surface, and recognized as the key fabrication tools for nano-electronics devices such as single electron transistors (SETs). For this purpose, the atomic force microscope (AFM) tip-induced oxides were used as etch masks to demonstrate a Si metal-oxide-semiconductor field-effect transistors (MOSFET),[1] and a side-gated FET.[2] More recently, the AFM tip-induced oxide patterns were used as the integral parts of room temperature operable SETs in Ti,[3] and Nb.[4]

Our research interest lies in the development of SPM tip-induced local oxidation technique, suited for the compound semiconductor heterostructures such as GaAs/AlGaAs,[5] and GaAs/InAs.[6] This is because one can make use of high electron mobility two-dimensional electron gas systems, which can be reliably fabricated with the current epitaxial growth technology like the molecular beam epitaxy (MBE). Further, the embedded structures as such are generally advantageous over the metal-based devices from a practical viewpoint, since the active region is not exposed to the surface and prevented from the mechanical damage. To this effort, we have previously demonstrated that the nano-scale AlGaAs/GaAs oxides generated by the AFM tip-induced oxidation process can be used as the integral tunnel barriers required for single electron transport. Such devices were shown to be stable and operable up to elevated temperatures,[7, 8] which can thus be regarded as one important step toward the development of nano-electronics devices.

In order to widely employ the local probe nano-oxidation process, however, it is necessary that one clearly understand the mechanisms and kinetics of the oxidation process for precise control. In addition, the properties and stability of the AFM-generated oxides should also be investigated. Though several groups have performed some detailed studies on the SPM tip-induced oxidation of Si,[9-11] much is still to be explored for GaAs/AlGaAs system.[5] In this work, we have attempted to determine some of the basic properties of the tip-generated GaAs oxides.

## 2. EXPERIMENTAL

Local tip-induced oxidation was performed in air at room temperature using a commercially available SPM system on freshly etched $n^+$-GaAs(100) (Si-doped to ~ 1 × $10^{18}$ $cm^{-3}$) substrates.[6] The contact-mode doped $n^+$-Si AFM tips were used, and the ambient humidity was maintained at ~ 45% by normal air conditioning. The feedback electronics control was turned on during the oxidation so that the contact force was kept constant.

For the XPS (X-ray photoelectron spectroscopy) analysis, a computer script directed the AFM to generate a total oxidized area of ~ 7.0 μm × 7.0 μm in a GaAs substrate. The tip bias and scan speed were −12 V and 0.1 μm/s, respectively. The average oxide height in the tip-oxidized area was measured to be ~ 2.0 nm. After loading the sample into a scanning XPS microprobe system, the spectrometer was pumped down to a base pressure of ~ 3× $10^{-9}$ Torr. The XPS spectra were then recorded using an Al Kα (1486.6 eV) radiation line and the beam diameter was ~ 5.0 μm.

## 3. RESULTS AND DISCUSSION

### 3.1. XPS analysis of AFM tip-induced GaAs oxides

Figure 1 shows the measured XPS spectra detected at an ejection angle of 45° for the Ga-3d and As-3d core levels after sputtering the surface by a thickness of ~ 1.0 nm by an $Ar^+$ beam, and three features are hereby noted. Firstly, it is known that the peak XPS signal observed at ~ 19.1 eV is from Ga bounded in GaAs, and one at ~ 41.1 eV is from As bounded in GaAs, respectively.[12] The additional peaks, one at ~ 20.2 eV of Ga-3d can be attributed to $Ga_2O_3$,[13] and another at ~ 44.1 eV of As-3d can be assigned as $As_2O_3$. Neither elemental arsenic nor advanced oxides were resolvable in these spectra, and thus $Ga_2O_3$ and $As_2O_3$ are regarded to be the main oxide constituents. Secondly, while the Ga and As oxide-related peaks due to the native oxide were not observed from the un-oxidized area after sputtering, these oxide-related peaks from the anodic oxides were clearly observable from the tip-oxidized region. Thirdly, the integrated signal ratio of $Ga_2O_3/As_2O_3$ determined for the tip-induced oxide region after 1.0 nm sputtering was > 1.5. If an ideal anodic reaction of GaAs was considered,

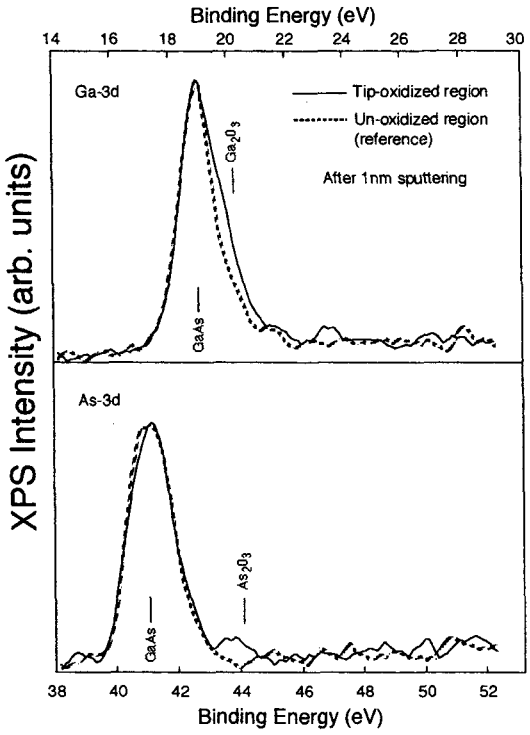


Fig. 1: XPS spectra measured for the Ga-3d and As-3d core levels after sputtering the as-received substrate surface by a thickness of ~ 1.0 nm.

$$GaAs + 3OH^- \rightarrow \frac{1}{2}Ga_2O_3 + \frac{1}{2}As_2O_3 + \frac{3}{2}H_2 + 3e^-$$

then 1 mole of GaAs forms a 1/2 mole of $x$ ($Ga_2O_3$) + $y$ ($As_2O_3$), and $x$ / $y$ = 1 would be satisfied. However, the XPS results showed that the AFM tip-generated GaAs oxide was slightly $Ga_2O_3$-rich. This is, however, not unreasonable because of the dissoluble and volatile nature of $As_2O_3$.[14] It has also been reported that $As_2O_3$ in contact with GaAs would undergo a reaction to yield $Ga_2O_3$ and elemental As at the interface.[15]

3.2. Electrical characterization of AFM tip-induced GaAs oxides

A GaAs oxide nano-dot was generated by holding the tip stationary at a given point on the substrate surface and applying a DC bias of –8 V for 10s. Figure 2 shows the typical current flow behavior measured during the tip-induced oxidation. An initial large current dropped rapidly within ~ 5s, after which small changes in the monitored current at ~ 0.5 nA were observed. This suggested that the oxidation in the proximity of tip apex was practically complete within 5s after application of bias. This is due to the self-limiting influence of the decreasing electric field, and the oxide practically ceases to grow for the electric field strength < ~$1\times10^7$ Vcm$^{-1}$.[5,10]

Figure 3(a) shows the *I–V* curve measured across the GaAs oxide nano-dot over a bias range of $V = 0 \sim 3.0$ V, and a modified Fowler-Nordheim (FN) plot,[16] of ln ( $I$ / $V^2$) *vs.* 1 / $V$ of the *I–V* curve (a) is shown in Fig. 3(b), respectively. Here it was assumed that (1) all the applied

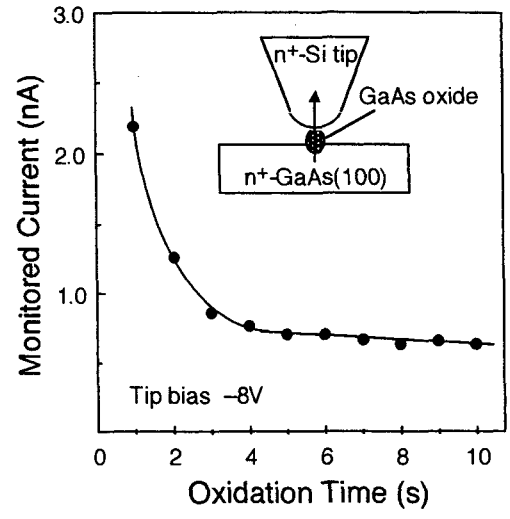


Fig. 2: Measured current during the tip-induced oxidation. An initial large current dropped sharply within ~ 5s, after which it reached a steady state with small changes in the current at ~ 0.5 nA.

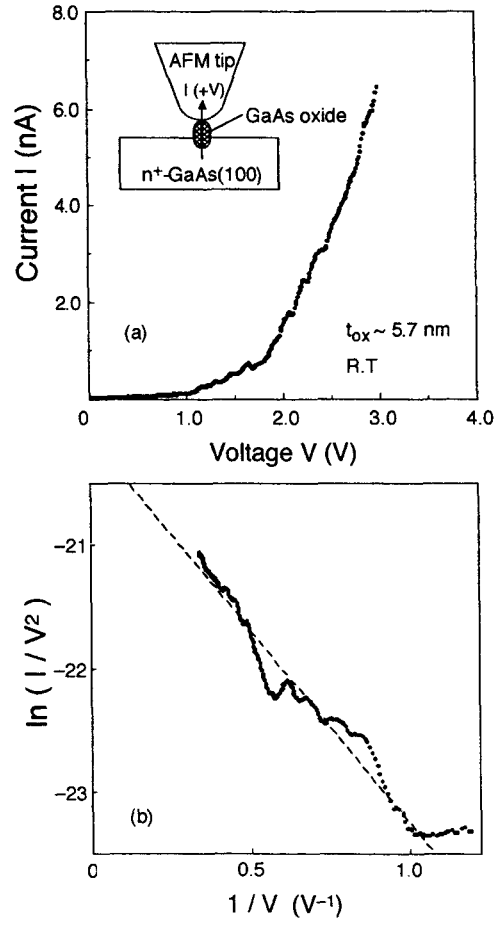


Fig. 3 (a) *I–V* curve measured across a GaAs oxide nano-dot, and (b) modified Fowler-Nordheim (FN) plot of ln ($I$ /$V^2$) *vs.* 1 / $V$ of the *I–V* curve shown in (a), respectively.

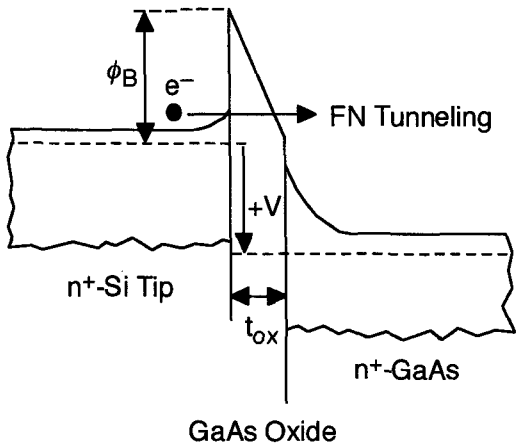


Fig. 4: Schematic illustration of energy band diagram for $n^+$-Si tip / tip-induced GaAs anodic oxide / $n^+$-GaAs junction in the high FN bias range ($V > 0$).

bias drops across the GaAs anodic oxide, (2) native oxide on the surface of the doped-Si tip is small compared to GaAs oxide thickness, and (3) GaAs anodic oxide thickness is given by $t_{ox} \sim 1.5\ h_{ox}$,[5] and hence $t_{ox}$ = 5.7 nm, where $h_{ox}$ is the oxide height measured by AFM. The GaAs oxide nano-dot diameter was ~ 50 nm. It can be seen from Fig. 3(b) that the FN plot follows a linear relationship in the high bias range, and hence the electron transport across the GaAs oxide nano-dot, from the doped-Si tip into GaAs substrate, is due to the FN tunneling mechanism. Therefore, the energy band diagram for the $n^+$-Si tip / tip-induced GaAs oxide / $n^+$-GaAs junction in the high (FN) bias range ($V > 0$) can be schematically illustrated as shown in Fig. 4. On the other hand, the current before the tip-induced oxidation did not follow the FN tunneling model. Though there existed a thin layer of native oxide on the substrate surface, typically < 1.0 nm as based on the XPS data, the current across such a thin oxide was expected to be due to the direct tunneling mechanism.[17] The barrier height $\phi_B$ can also be determined from the slope of FN plot as shown in Fig. 3(b). As a crude estimate, by using $m_e^* = 0.2\ m_0$ ( $m_0$ is the free electron mass) reported in the literature,[18] $\phi_B$ in the high (FN) bias range ($V > 0$) of ~ 0.32 eV can be obtained.

## 4. Summary

The main purpose of this work was to evaluate some of the basic properties of the GaAs oxide generated by the local probe nano-oxidation process. The chemical analysis using the scanning microprobe XPS has revealed that the main constituents of the AFM tip-generated GaAs oxides were $Ga_2O_3$ and $As_2O_3$. Next, the *I–V* characterization has shown that the electronic flow across the GaAs oxide dot of ~ 5.7 nm thickness, from the doped-Si tip into GaAs substrate over a range of applied bias, was due to the Fowler-Nordheim tunneling mechanism. $\phi_B$ in the high (FN) bias range ($V > 0$) of ~ 0.32 eV was obtained as a rough estimate. Lastly, the authors would like to gratefully acknowledge Professor J. S. Harris of Stanford University for his continuing support.

References

[1] S. C. Minne, H. T. Soh, P. Flueckinger, and C. F. Quate, *Appl. Phys. Lett.*, **66**, 703 (1995).
[2] P. M. Campbell, E. S. Snow, and P. J. McMarr, *Appl. Phys. Lett.*, **66**, 1388 (1995).
[3] K. Matsumoto, M. Ishii, K. Segawa, Y. Oka, B .J. Vartanian, and J. S. Harris, *Appl. Phys. Lett.*, **68**, 34 (1996).
[4] J. Shirakashi, K. Matsumoto, N. Miura, and M. Konagai, *Appl. Phys. Lett.*, **72**, 1893 (1998).
[5] Y. Okada, S. Amano, M. Kawabe, and J. S. Harris, Jr., *J. Appl. Phys.*, **83**, 7998 (1998).
[6] Y. Okada, S. Amano, M. Kawabe, B. N. Shimbo, and J. S. Harris, Jr., *J. Appl. Phys.*, **83**, 1844 (1998).
[7] Y. Okada, S. Amano, Y. Iuchi, and M. Kawabe, and J. S. Harris, Jr., *Electron. Lett.*, **34**, 1262 (1998).
[8] Y. Okada, Y. Iuchi, and M. Kawabe, and J. S. Harris, Jr., *Jpn. J. Appl. Phys.*, **38**, L160 (1999).
[9] D. Stiévenard, P. A. Fontaine, and E. Dubois, *Appl. Phys. Lett.*, **70**, 3272 (1997).
[10] Ph. Avouris, T. Hertel, and R. Martel, *Appl. Phys. Lett.*, **71**, 285 (1997).
[11] Ph. Avouris, R. Martel, T. Hertel, and R. Sandstrom, *Appl. Phys. A*, **66**, S659 (1998).
[12] H. Iwasaki, Y. Mizokawa, R. Nishitani, and S. Nakamura, *Surf. Sci.*, **86**, 811 (1979).
[13] G. P. Schwartz, G. J. Gualtieri, G. W. Kammoltt, and B. Schwartz, *J. Electrochem. Soc.*, **126**, 1737 (1979).
[14] H. Wang, C. Huang, Y. Wang, and M. Houng, *Jpn. J. Appl. Phys.*, **37**, L67 (1998).
[15] C. D. Thurmond, G. P. Schwartz, G. W. Kammoltt, and B. Schwartz, *J. Electrochem. Soc.*, **127** 1366 (1980).
[16] M. Lenzlinger and E. H. Snow, *J. Appl. Phys.*, **40**, 278 (1969).
[17] T. Yasue, H. Koyama, T. Kato, and T. Nishioka, *J. Vac. Sci. Technol. B*, **15**, 614 (1997).
[18] I. Hase, H. Kawai, K. Kaneko, and N. Watanabe, *J. Appl. Phys.*, **59**, 3792 (1986).

(Received December 17, 1999; Accepted March 30, 2000)